

# Dynamic Response of Functionally Graded Circular Plate under Thermal Shock

Jing-Hua ZHANG<sup>1,a</sup>, Shuang-Chao PAN<sup>1,b,\*</sup>

<sup>1</sup>School of Sciences, Lanzhou University of Technology, Lanzhou 730050, China

<sup>a</sup>zjhhrb@163.com, <sup>b</sup>shch\_pan@sina.com

\*Corresponding author

**Keywords:** Functionally Graded Materials, Circular Plate, Thermal Shock, Dynamic Response.

**Abstract.** Dynamic response of a functionally graded material circular plate subjected to thermal shock is investigated based on the von Kármán's plate theory. The geometric imperfections of the plate are taken into account and the bottom surface of the circular plate is subjected to uniform thermal shock loadings. The deflections of dynamic response are obtained by numerically solving the governing equations using series expansions and Runge-Kutta method. The effects of the material constitution and initial geometric imperfection of the plate on the dynamic response are discussed.

## Introduction

Comprehensive works on the transient response of structures under thermal shock have been reported in the literature. Most of these researches are involved the conventional composite materials or homogeneous materials. Huang and Duan[1] studied the dynamic buckling of a circular copper plate under laser irradiation. Based on the fully coupled thermoelastic theory, thermal dynamic stability of symmetrically laminated orthotropic rectangular plates subjected to an oscillating thermal load was analyzed by Markus, et al. [2].

Functionally graded materials (FGM) have been regarded as one of the advanced inhomogeneous composite materials, usually made from metal and ceramic, taking advantage of the merits of constituent materials adequately. However, there have been few researches involving dynamic stability of FGM structures under thermal shock. Based on the classical shell theory with Sanders' nonlinear kinematic relations, a dynamic thermal post-buckling behavior of functionally graded cylindrical shells subjected to the combined action of thermal load and applied actuator voltage was analyzed by Mirzavand, et al. [3]. A finite difference based method combined with the Runge-Kutta method was employed to predict the post-buckling equilibrium paths. On the basis of the third-order shear deformation shell theory, Mirzavand, et al. [4] obtained the piezoelectric functionally graded cylindrical shell buckling equilibrium paths and dynamic buckling temperature. Mehrian and Naei[5] studied dynamic response of functionally graded partial annular disk under radial thermal shock by using a hybrid Fourier-Laplace transform in conjunction with finite element approach.

In the present paper, the dynamic response of imperfect circular FGM plates under thermal shock is investigated. Some regular conclusions are achieved through analyzing and discussing the numerical solutions in detail.

## Problem Formulation

### Material Properties of the FGM Plate

We consider a circular functionally graded plate with uniform thickness  $h$ , radius  $R$ . The mid-plane of the plate is referred to cylindrical coordinates  $r$  and  $\theta$  in the radial and the circumferential directions. Thickness direction coordinate is  $z$ , positive upward. The material properties of the FGM plate are assumed to vary only in the thickness direction from full metal at the top surface to full ceramic at the bottom. The volume fractions and material properties are

$$V_c(z) = \left( \frac{h-2z}{2h} \right)^n, V_m(z) = 1 - V_c, P(z) = (P_c - P_m)V_m(z) + P_m. \quad (1)$$

Where  $P_c$  and  $P_m$  are material properties of ceramic and metal, respectively.  $V_c(z)$  is the volume content of the ceramic,  $k$  is the volume fraction index of the ceramic.

### Fundamental Equations

The corresponding displacements in the mid-surface of the circular plate are designated  $u(r, t)$  and  $w(r, t)$  in directions of  $r$  and  $z$ , respectively. Considering axisymmetric deformation, the displacement  $v$  in the direction of  $\theta$  is zero. Linear geometrical equations and constitutive equations are expressed as

$$\{\varepsilon_r, \varepsilon_\theta\}^T = \{\varepsilon_r^0, \varepsilon_\theta^0\}^T + z \{\kappa_r, \kappa_\theta\}^T, \quad (2a)$$

$$\{\varepsilon_r^0, \varepsilon_\theta^0\}^T = \left\{ \frac{\partial u}{\partial r} + \frac{\partial w}{\partial r} \frac{\partial w_0}{\partial r} + \frac{1}{2} \left( \frac{\partial w}{\partial r} \right)^2, \frac{u}{r} \right\}^T, \quad \{\kappa_r, \kappa_\theta\}^T = \left\{ -\frac{\partial^2 w}{\partial r^2}, -\frac{1}{r} \frac{\partial w}{\partial r} \right\}^T, \quad (2b)$$

$$\sigma_r = \frac{E(z)(\varepsilon_r + \nu \varepsilon_\theta)}{1 - \nu^2} - \frac{E(z)\alpha(z)T(z, t)}{1 - \nu}, \quad \sigma_\theta = \frac{E(z)(\varepsilon_\theta + \nu \varepsilon_r)}{1 - \nu^2} - \frac{E(z)\alpha(z)T(z, t)}{1 - \nu}. \quad (3a, b)$$

Where  $\varepsilon_r$  and  $\varepsilon_\theta$  are the normal strains at an arbitrary point in the mid-surface of the deformed plate,  $\kappa_r$  and  $\kappa_\theta$  are curvatures, produced by the deformation,  $w_0(r)$  is the initial geometric imperfection,  $t$  is the time,  $\sigma_r$  and  $\sigma_\theta$  are the normal stresses in  $r$  and  $\theta$  directions, respectively.  $T(z, t)$  is the temperature rise.

Substituting Eqs.(2a, b) into Eqs.(3a, b), integrating  $\sigma_r$  and  $\sigma_\theta$  along the thickness direction, the membrane forces and the bending moments per unit area are given by

$$N_r = A(\varepsilon_r^0 + \nu \varepsilon_\theta^0) + B(\kappa_r + \nu \kappa_\theta) - N^T, \quad N_\theta = A(\varepsilon_\theta^0 + \nu \varepsilon_r^0) + B(\kappa_\theta + \nu \kappa_r) - N^T, \quad (4a)$$

$$M_r = B(\varepsilon_r^0 + \nu \varepsilon_\theta^0) + D(\kappa_r + \nu \kappa_\theta) - M^T, \quad M_\theta = B(\varepsilon_\theta^0 + \nu \varepsilon_r^0) + D(\kappa_\theta + \nu \kappa_r) - M^T. \quad (4b)$$

$$\text{where } (A, B, D) = \frac{1}{1 - \nu^2} \int_{-h/2}^{h/2} E(z) (1, z, z^2) dz, \quad (N^T, M^T) = \frac{1}{1 - \nu} \int_{-h/2}^{h/2} E(z) \alpha(z) T(z, t) (1, z) dz.$$

### The Transient Temperature Field

The dynamic response of FGM circular plate under the initial steady-state heat balance environment and suddenly subjected to uniform thermal loads on its lower surface is investigated. The temperature field of the plate varies with time and the location of the thickness direction, and its upper surface exchanges heat with the external environment. Thus, the heat conduction equation in the absence of internal heat sources reduces to

$$C(z)\rho(z) \frac{\partial T}{\partial t} = \frac{\partial}{\partial z} \left[ K(z) \frac{\partial T}{\partial z} \right], \quad \left( t > 0, -\frac{h}{2} < z < \frac{h}{2} \right). \quad (5)$$

The thermal initial conditions and the boundary conditions on the lower and the upper surfaces, are specified as

$$T(z, 0) = 0, \quad T\left(-\frac{h}{2}, t\right) = (\Delta T)(1 - e^{-at}), \quad -K(z) \frac{\partial T}{\partial z} \Big|_{z=h/2} = h_r T\left(\frac{h}{2}, t\right). \quad (6)$$

Where  $h_r$  is the heat exchange coefficient between the upper surface of the plate and the environment.

The Laplace transformation technique and the power series method are employed to solve Eqs(5, 6) so the temperature can be obtained.

### Motion Equations and Dynamic Governing Equations

Equilibrium equations of the circular plate with axisymmetric deformations are derived in terms of the resultant forces as follows:

$$\frac{\partial(rN_r)}{\partial r} - N_\theta = 0, \quad \frac{\partial^2(rM_r)}{\partial r^2} - \frac{\partial M_\theta}{\partial r} + \frac{\partial}{\partial r} \left( rN_r \left( \frac{\partial w}{\partial r} \right) \right) - I_0 r \frac{\partial^2 w}{\partial t^2} = 0 \quad (7a, b)$$

Where  $I_0 = \int_{-h/2}^{h/2} \rho(z) dz$  is the mass per unit area.

Substitute Eqs. (2a, b), (4a, b) into Eqs. (7a, b) and introduce the following dimensionless quantities for an easy solution.

$$x = \frac{r}{R}, \quad (W, W_0) = \frac{(w, w_0)}{h}, \quad \tau = t \sqrt{\frac{E_m}{\rho_m h^2}}, \quad U = \frac{uR}{h^2}, \quad D_1 = \frac{A}{hE_m}, \quad D_2 = \frac{B}{h^2 E_m}, \quad D_3 = \frac{D}{h^3 E_m}, \quad D_4 = \frac{h}{R},$$

$$N_T = \frac{N^T R^2}{E_m h^3}.$$

Where  $E_m$  is the Young's modulus of metal material. Therefore, the dimensionless governing equations are

$$\frac{\partial}{\partial x} \left[ \frac{1}{x} \frac{\partial}{\partial x} (xU) \right] = \frac{D_2}{D_1} F_1 + F_2, \quad D_3 \nabla^4 W = -N_T F_3 + D_2 (F_4 + F_5) + D_1 (F_6 + F_7) - \frac{D_0}{D_4^4} \frac{\partial^2 W}{\partial \tau^2}. \quad (8a, b)$$

in which the linear differential operators  $\nabla^4 = \frac{\partial^4}{\partial x^4} + \frac{2}{x} \frac{\partial^3}{\partial x^3} - \frac{1}{x^2} \frac{\partial^2}{\partial x^2} + \frac{1}{x^3} \frac{\partial}{\partial x}$ ,  $F_1 \sim F_7$  are partial differential expressions of  $U$  and  $W$ , given in the Appendix.

The edge of the plate considered is simply supported, so the dimensionless boundary conditions at the edge and the continuous conditions at the center of the plate are written as

$$x=0: U=0, \quad W=\delta, \quad \frac{\partial W}{\partial x}=0, \quad \lim_{x \rightarrow 0} \left( \frac{1}{x} \frac{d^2 W}{dx^2} + \frac{d^3 W}{dx^3} \right) = 0, \quad x=1: W=0, \quad U=0, \quad \frac{\partial^2 W}{\partial x^2} = 0 \quad (9a, b)$$

Assume that the circular FGM plate axisymmetric deflection of expression is a power series[1], this is

$$W = \delta \left( 1 + \sum_{i=2,4}^{\infty} A_i x^i \right) \approx \delta (1 + A_2 x^2 + A_4 x^4), \quad W_0 = \delta_0 (1 + A_2 x^2 + A_4 x^4). \quad (10a, b)$$

Where simply supported edge  $A_2 = -\frac{2(3+\nu)}{5+\nu}$ ,  $A_4 = -\frac{1+\nu}{5+\nu}$ ,  $\delta$ ,  $\delta_0$  is the maximum deflection and initial deflection at the center point of plate.

Substituting Eqs.(10a, b) into Eqs.(8a, b), and integrating the dimensionless governing equations, yields

$$U = \eta_1 \delta^2 + \eta_2 \delta + C_1 x + \frac{C_2}{x}, \quad (11a)$$

$$D_3 D_4 W = \lambda_1 \delta^3 + \lambda_2 \delta^2 + \lambda_3 \delta + \lambda_4 \ddot{\delta} + \lambda_5 + \frac{C_3 x^2 (\ln x - 1)}{4} + \frac{C_4 x^2}{4} + C_5 \ln x + C_6. \quad (11b)$$

Where  $C_1 \sim C_6$  are constants of integration,  $\eta_1$ ,  $\eta_2$ ,  $\lambda_1 \sim \lambda_5$  polynomial for  $x$ . Use the boundary conditions  $U=0$  at  $x=0$  and  $x=1$ , we have

$$C_1 = \left[ \frac{(7-\nu)A_4^2}{6} + \frac{(5-\nu)A_2A_4}{3} + \frac{(3-\nu)A_2^2}{4} \right] \delta^2 + \left( \frac{(3-\nu)A_2^2}{2} + \frac{(7-\nu)A_4^2}{3} + \frac{(10-2\nu)A_2A_4}{3} \right) \delta_0 \delta - \frac{4D_2A_4}{D_1} \delta,$$

$$C_2 = 0.$$

Substituting Eq.(11a) into Eq.(11b), in view of the finiteness of  $W = \delta$  and  $\lim_{x \rightarrow 0} \left( \frac{1}{x} \frac{d^2W}{dx^2} + \frac{d^3W}{dx^3} \right) = 0$  at  $x=0$ , we have  $C_3 = 0$ ,  $C_5 = 0$ .

Use the boundary conditions at  $x=1$  will be  $W = 0$ ,  $\frac{\partial^2 W}{\partial x^2} = 0$ , we obtained

$$C_4 = B_1\delta^3 + B_2\delta^2 + B_3\delta + B_4 + B_5\ddot{\delta}, \quad C_6 = B_6\delta^3 + B_7\delta^2 + B_8\delta + B_9 + B_{10}\ddot{\delta}.$$

Detailed expressions of polynomial  $B_1 \sim B_{10}$  are given in the Appendix. The Eqs.(11b) will be solved numerically by using Runge-Kutta method.

### Numerical Results and Discussions

In the computation, a circular FGM plate made of the constituents of SiC and Ni is considered. Poisson's ratio of the plate is constant and specified as  $\nu = 0.3$ . The material properties of the constituents are reference to literature [6]. The geometries of the FGM circular plate are  $R = 0.2\text{m}$ ,  $h = 0.01\text{m}$ . The lower surface is subjected to thermal shock loading  $T(-h/2, t) = \Delta T(1 - e^{-at})$ , here  $\Delta T = 300\text{K}$ ,  $a = 10$ . Given the heat exchange coefficient is  $h_r = 50$ .

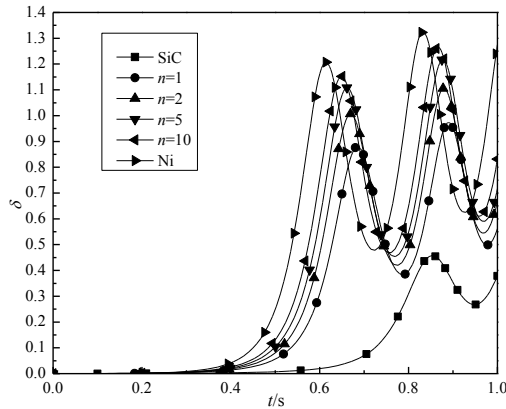


Fig. 1 The Central Deflection Responses of the FGM Circular Plate with Different  $n$

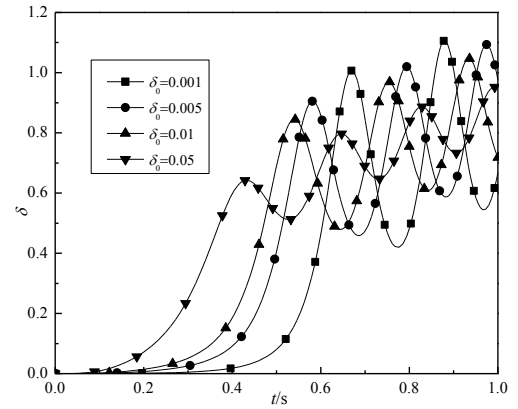


Fig. 2 The Central Deflection Responses of the FGM Circular Plate for Some Specified Imperfections

For some specified values of volume fraction index  $n$  at  $\delta_0 = 0.001$ , Fig.1 shows the transient central deflections in the middle surfaces of the FGM circular plate under thermal shock. The maximum central deflections of the metal and ceramic FGM circular plate are intermediate to those of the metal and the ceramic plate and increase monotonously with the increasing of volume fraction index  $n$  for thermal shock. Given value of power law index  $n=2$ , Fig.2 shows the dynamic response of the plate is very sensitive to the magnitude of the initial imperfect. Similar discussions can be found in literatures [1, 6].

### Summary

Dynamic response of a functionally graded material circular plate subjected to thermal shock is investigated by using the series expansions technical and Runge-Kutta method. It is found that the maximum central deflections increase monotonously with the increasing of volume fraction index  $n$  for thermal shock. The ability of the structure to withstand thermal shock is reduced with the increasing of

power law index  $n$ . And the dynamic response of the plate is very sensitive to the magnitude of the initial imperfect.

## Acknowledgement

This work was financially supported by the National Natural Science Foundation of China (Nos.11262010,11272278). The authors gratefully acknowledge the support.

## References

- [1]C. G. Huang, Z.P. Duan, Studies on the dynamic buckling of circular plate irradiated by laser beam [J], Applied Mathematics and Mechanics. 23 (2002) 667-672.
- [2]S. Markus, J.B. Greenberg, Y. Stavsky, Coupled thermoelastic theory for dynamic stability of composite plates [J], Journal of Thermal Stresses. 18 (1995) 335-357.
- [3]B. Mirzavand, M.R. Eslami, M. Shakeri, Dynamic thermal postbuckling analysis of piezoelectric functionally graded cylindrical shells [J], Journal of Thermal Stresses. 33 (2010) 646-660.
- [4]B. Mirzavand, M.R. Eslami, J.N. Reddy, Dynamic thermal postbuckling analysis of shear deformable Piezoelectric-FGM cylindrical shells [J], Journal of Thermal Stresses. 36 (2013) 189-206.
- [5]S.M.N. Mehrian, M. H. Naei, Two dimensional analysis of functionally graded partial annular disk under radial thermal shock using hybrid Fourier-Laplace transform [J], Applied Mechanics and Materials. 436 (2013) 92-99.
- [6]S.R. Li, L.L. Fan, Dynamic responses of functionally graded material beams under thermal shock [J], Journal of Vibration Engineering. 22 (2009) 371-378(in Chinese).

## Appendix

$$\begin{aligned}
 F_1 &= \frac{\partial^3 W}{\partial x^3} + \frac{1}{x} \frac{\partial^2 W}{\partial x^2} - \frac{1}{x^2} \frac{\partial W}{\partial x}, F_2 = -\left( \frac{\partial^2 W}{\partial x^2} - \frac{\partial^2 W_0}{\partial x^2} + \frac{1-\nu}{2x} \frac{\partial W}{\partial x} \right) \frac{\partial W}{\partial x} - \left( \frac{\partial^2 W}{\partial x^2} + \frac{1-\nu}{x} \frac{\partial W}{\partial x} \right) \frac{\partial W_0}{\partial x}, \\
 F_3 &= \frac{\partial^2 W}{\partial x^2} + \frac{\partial^2 W_0}{\partial x^2} + \frac{1}{x} \left( \frac{\partial W}{\partial x} + \frac{\partial W_0}{\partial x} \right), F_4 = \frac{1}{x} \frac{\partial}{\partial x} x \frac{\partial}{\partial x} \frac{1}{x} \frac{\partial}{\partial x} (xU), \\
 F_5 &= \frac{1-3\nu}{x} \frac{\partial W}{\partial x} \frac{\partial^2 W}{\partial x^2} + \frac{1-2\nu}{x} \frac{\partial^2 W}{\partial x^2} \frac{\partial W_0}{\partial x} + \left[ \frac{2(1-\nu)}{x} \frac{\partial W}{\partial x} + \frac{\partial^2 W}{\partial x^2} \right] \frac{\partial^2 W_0}{\partial x^2} + \frac{\partial W}{\partial x} \frac{\partial^3 W_0}{\partial x^3}, \\
 F_6 &= \frac{1}{x} \frac{\partial}{\partial x} \left[ x \left( \frac{\partial U}{\partial x} + \frac{\nu}{x} U \right) \frac{\partial W}{\partial x} \right] + \left[ \frac{\partial U}{\partial x} + \frac{\nu}{x} U \right] \frac{\partial^2 W_0}{\partial x^2} + \left( \frac{\partial^2 U}{\partial x^2} + \frac{1+\nu}{x} \frac{\partial U}{\partial x} \right) \frac{\partial W_0}{\partial x}, \\
 F_7 &= \frac{1}{x} \frac{\partial}{\partial x} \left[ \frac{x}{2} \left( \frac{\partial W}{\partial x} \right)^2 \frac{\partial W}{\partial x} \right] + \left( 2 \frac{\partial W_0}{\partial x} + \frac{3}{2} \frac{\partial W}{\partial x} \right) \frac{\partial W}{\partial x} \frac{\partial^2 W_0}{\partial x^2} + \left( 3 \frac{\partial W}{\partial x} + \frac{\partial W_0}{\partial x} \right) \frac{\partial^2 W}{\partial x^2} \frac{\partial W_0}{\partial x} \\
 &\quad + \left( \frac{3}{2x} \frac{\partial W}{\partial x} + \frac{1}{x} \frac{\partial W_0}{\partial x} \right) \frac{\partial W}{\partial x} \frac{\partial W_0}{\partial x}, \\
 B_1 &= \left( 0.208 A_2^2 + 0.375 A_4^2 - 0.953 - 0.375 \nu^2 A_4^2 - 0.953 \nu - 0.208 \nu^2 A_2^2 \right) D_1 D_4^4 A_2 \\
 &\quad + \left( 0.486 A_2^2 - 1.059 \nu - 0.122 \nu^2 A_4^2 - 0.486 \nu^2 A_2^2 - 1.059 + 0.122 A_4^2 \right) D_1 D_4^4 A_4
 \end{aligned}$$

$$\begin{aligned}
B_2 &= \left(0.367A_4^2 - 3.177\nu + 1.125A_2A_4 - 3.177 + 1.458A_2^2 - 1.458A_2^2\nu^2 - 0.367A_4^3\nu^2\right)D_1D_4^4A_4\delta_0 \\
&\quad + \left(0.625A_2^2 - 1.125A_4^2\nu^2 - 0.625A_2^2\nu^2\right)D_1D_4^4A_2\delta_0 + (1.635 + 1.635\nu + 3.333A_2\nu)D_2D_4^4A_4 \\
&\quad + (1.472 + 3A_2 - 2.859\nu\delta_0 + 3A_2\nu - 2.859\delta_0 + 1.472\nu + 3.333A_4)D_2D_4^4A_2 \\
B_3 &= \left[0.972A_2A_4 + 0.417A_2^2(1-\nu^2) + 0.75A_4^2(1-\nu^2) - 1.906(\nu+1)\right]D_1D_4^4A_2\delta_0^2 - \frac{24D_2D_4^4A_4}{D_1} \\
&\quad + \left[0.244A_4^2(1-\nu^2) - 0.972A_2^2\nu^2 - 2.118(\nu+1)\right]D_1D_4^4A_4\delta_0^2 + (1.5A_2 + 1.667A_4)D_4^4N_T \\
&\quad + \left[3A_2(\nu+1) + 1.477 + 3.333A_4(\nu+1) + 1.472\nu\right]D_2D_4^4A_2\delta_0 + 1.635(\nu+1)D_2D_4^4A_4\delta_0 \\
B_4 &= 1.667A_4D_4^4\delta_0N_T + 1.5A_2D_4^4\delta_0N_T, \quad B_5 = 0.375D_0 + 0.104D_0A_2 + 0.049D_0A_4, \\
B_6 &= \left(0.199\nu + 0.049\nu^2A_2^2 - 0.049A_2^2 - 0.092A_4^2 + 0.199 + 0.092\nu^2A_4^2 - 0.117A_2A_4\right)D_1D_4^4A_2 \\
&\quad + \left(0.247\nu + 0.03\nu^2A_4^2 + 0.0117\nu^2A_2^2 + 0.247 - 0.03A_4^2\right)D_1D_4^4A_4, \\
B_7 &= \left[(0.146A_2^2 + 0.275A_4^2)(\nu^2 - 1) + 0.596(\nu+1) + 0.352A_2A_4\nu^2\right]D_1D_4^4A_2\delta_0 - 0.352A_2^2D_1D_4^4A_4\delta_0 \\
&\quad + \left[0.741(\nu+1) + 0.09A_4^2(\nu^2 - 1)\right]D_1D_4^4A_4\delta_0 - \left[(0.625A_2 + 0.307)(\nu+1) + 0.778A_4\right]D_2D_4^4A_2 \\
&\quad - \left[0.382(\nu+1) + 0.778A_2\nu\right]D_2D_4^4A_4 \\
B_8 &= \left[0.397(\nu+1) + 0.097A_2^2(\nu^2 + 1) + 0.183(\nu^2 - 1)A_4^2\right]D_1D_4^4A_2\delta_0^2 - (0.313A_2 - 0.389A_4)D_4^4N_T \\
&\quad + \left(0.06A_4^2 + 0.234A_2^2\right)(\nu^2 - 1)D_1D_4^4\delta_0^2A_4 + (0.494\delta_0 - 0.382)(\nu+1)D_1D_4^4A_4\delta_0 + \frac{5D_2^2D_4^4A_4}{D_1} \\
&\quad - (0.307 + 0.625A_2 + 0.778A_4)(\nu+1)D_2D_4^4A_2\delta_0, \\
B_9 &= 0.389A_4D_4^4\delta_0N_T + 0.313A_2D_4^4\delta_0N_T, \quad B_{10} = 0.078D_0 + 0.024D_0A_2 + 0.112D_0A_4.
\end{aligned}$$